

Cite this: *RSC Adv.*, 2017, 7, 55264Received 9th November 2017
Accepted 30th November 2017

DOI: 10.1039/c7ra12281k

rsc.li/rsc-advances

Mass spectrometry and potentiometry studies of Al(III)–naringin complexes†

L. Bartella, E. Furia * and L. Di Donna

Here we have studied the complexation of naringin with Al(III) under physiological conditions (*i.e.*, at 37 °C and in 0.16 mol L⁻¹ NaCl). Solubility and protonation constants of the ligand were first determined in order to evaluate the competition of naringin for the Al(III) and H⁺ ions. Speciation analysis made by potentiometric titrations and supported by UV data shows that a complexation occurs at a 1 : 1 ligand-to-Al(III) stoichiometric ratio. Notably, these data combined with mass spectrometry results indicate that the complexation site is located on the β-hydroxy ketone moiety.

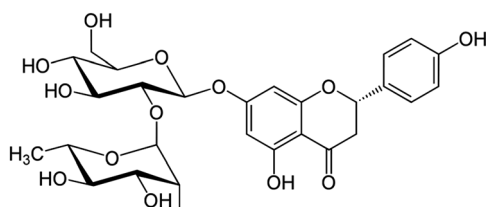
Introduction

Several biological effects, including radical scavenging and metal chelation, are ascribed to polyphenolic compounds. Numerous epidemiological studies have shown a correlation between high dietary intakes of phenolics and reduced risk of cardiovascular disease and cancer.^{1–5} Flavonoids, which contain a large group of polyphenolic phytochemicals with great therapeutic properties, have received much attention in the treatment of some diseases such as cancer, viral infection and inflammation. Most of their pharmacological activities are associated with enzymatic inhibition, anticancer and antioxidant activity and interference with reactions such as the formations of free radicals.^{6–9} Flavonoids are naturally present in vegetables, fruits, and beverages such as tea and wine. *In vitro*, flavonoids inhibit the oxidation of low-density lipoprotein and reduce thrombotic tendency, but their effects on atherosclerotic complications in human beings are unknown. Naringin (4',5,7-trihydroxy flavanone, HL, Scheme 1) is the major

flavonoid in grapefruit; due to its metal chelating, antiulcer, antioxidant, superoxide scavenging and anti-inflammatory properties, this compound has attracted scientific interest.^{10–13}

In our continuous investigation on the complexation behaviour of biological ligands towards some bioavailable metal cations,^{14–19} the purpose of this work was to study the sequestering ability of naringin with respect to aluminium cation under physiological conditions (*i.e.*, 37 °C and in 0.16 mol L⁻¹ NaCl). Solubility as well as acidic constant of naringin were determined under the same experimental conditions, too. Although the interaction of this compound with water is important because of its antioxidative activity in biological media involves water as the natural solvent, most of the studies reported in literature refers to measurements carried out in mixed solvents due to its low solubility in water.^{20–22}

The reason for choosing the aluminium cation is mainly due to the fact that human exposure to aluminium does not serve any essential function in human biochemistry. The aluminium cation can enter the brain where it persists for a long time causing neurotoxicity.²³ Some of the aluminium toxicity can be reduced by chelation, for this reason it was interesting to explore the sequestering ability of a natural product such as naringin to coordinate the Al(III) ion.



Scheme 1 Chemical structure of naringin.

Department of Chemistry and Chemical Technologies, University of Calabria, Via P. Bucci, Cubo 12/D, 87036, Arcavacata di Rende, CS, Italy. E-mail: emilia.furia@unical.it

† Electronic supplementary information (ESI) available: Fig. S1 relative to the further tandem mass spectrometry experiment performed on the isolated species at *m/z* 1185. Fig. S2 relative to the MS/MS spectrum of the other stable species at *m/z* 621. See DOI: 10.1039/c7ra12281k

Experimental

Materials

The hydrochloric acid and the sodium chloride stock solutions, and the sodium hydroxide titrant solutions were prepared and standardized as described in a previous work.²⁴ Aluminium(III) chloride stock solution was prepared and standardized as previously reported.¹⁸ Naringin (Sigma-Aldrich, ≥95%), used without further purification, was kept in a desiccator over silica gel. All solutions were prepared with bidistilled water.



Apparatus and experimental procedure

The potentiometric apparatus and Ag/AgCl electrodes were prepared as defined in a previous work.¹⁴ The glass electrodes, manufactured by Metrohm, acquired a constant potential within 10 min, after the addition of the reagents, that remained unchanged within ± 0.1 mV for several hours. The titrations were carried out with the same tool described in a previous work.¹⁵ To avoid the carbonate interference a slow stream of nitrogen gas was passed through three bottles (a–c) containing: (a) 1 mol L⁻¹ NaOH, (b) 1 mol L⁻¹ H₂SO₄ and (c) 0.16 mol L⁻¹ NaCl, and then into the test solutions, stirred during titrations, through the gas inlet tube. During the EMF measurements, the cell assembly was placed in a thermostat kept at (37.0 ± 0.1) °C.

The HPLC/UV analysis for the solubility measurements were performed by using a Fractionlynx HPLC system (Milford, MA) working in analytical mode equipped with a 2489 UV/Visible detector.²⁵ 20 μ L of naringin saturated solutions were injected into a C18 reverse phase Luna column 4.6×250 mm from Phenomenex (Torrance, CA). The run time was 25 min, and the elution gradient comprises the following step (mobile phase: solvent A: 0.1% HCOOH/H₂O, solvent: B CH₃OH): isocratic elution 80% A for 2 min; linear gradient from 80% A to 40% A in 10 min, isocratic elution 40% A for 2 min, linear gradient from 40% A to 20% A in 3 min; isocratic elution 20% A for 2 min; linear gradient from 20% A to 80% A in 3 min; equilibration of the column: 3 min. The area of the signal recorded at 280 nm wavelength, was matched to a calibration curve built analysing five standard solutions whose concentration ranged from 37.5 to 300 mg L⁻¹ in order to calculate the unknown concentration.

Information about the structure of complexes was gathered by recording the ESI MS and MS/MS spectra.²⁶ These were acquired by direct infusion of the solution (*i.e.*, naringin-aluminium complex at 60 mg kg⁻¹ concentration) into a Thermo Scientific TSQ Quantum Vantage triple-stage quadrupole mass spectrometer (Thermo Fisher Scientific, San José, CA). The mass spectrometer was equipped with a heated electrospray ionization (HESI II) source operating in positive ion mode. The experimental conditions were the following: spray voltage, 3.5 kV; vaporizer and capillary temperatures, 280 and 270 °C, respectively; sheath and auxiliary gas: 40 and 46 arbitrary units (au), respectively. The collision gas pressure (Ar) in the collision cell (Q2) was set at 1.0 mTorr, and the mass resolution at the first (Q1) and third (Q3) quadrupole was set at 0.7 Da (FWHM). The S-lens rf amplitude and the collision energy (CE) were 110 V and 50 eV, respectively.

Results and discussion

The complex formation equilibria between Al(III) and naringin were studied by measuring with a glass electrode the competition of the ligand for the aluminium(III) and H⁺ ions, using bidistilled water as solvent at 37.0 °C and in 0.16 mol L⁻¹ NaCl. The present study has provided, at first, the determination of the solubility and of the acidic constant of ligand under the selected experimental conditions. To evaluate the influence of ionic strength and ionic media on the solubility of naringin,

values at 37 °C were determined in pure water, in 1.0 and 3.0 mol L⁻¹ NaCl and in 0.5, 1.0 and 3.0 mol L⁻¹ NaClO₄, also. This knowledge is necessary when modelling the dependence of equilibrium constants on the ionic strength.

Solubility measurements

Solubility studies allow the determination of activity coefficients for nonelectrolyte solutes in aqueous solutions containing a large excess of salts, whose knowledge is necessary when modelling the dependence of equilibrium constants on ionic strength. It is well known from literature that the low solubilities in water of some solutes can be modified by the presence of cosolutes, such as inert salts, or by increasing the temperature.^{27–30} Two different phenomena related to solubility changes caused by the presence of cosolutes can be observed: salting-in and salting-out effects.³¹ Saturated naringin solutions were prepared as already described in a previous work.³² Briefly, solid was wrapped up in a highly retentive filter paper (Whatman 42) bag and then was kept in a glass cylinder containing pure water as well as sodium chloride aqueous solution at pre-established ionic strength values (*i.e.*, 0.16 mol L⁻¹), under continuous stirring with a magnetic bar. The cylinders were then placed in a thermostatic water bath at (37.0 ± 0.1) °C, and the naringin concentrations were monitored over time, until it reached a constant value, which usually occurred in about (7 to 10) days. Finally, the solubility values were obtained by analysing naringin saturated solutions by HPLC/UV. Results obtained at the different ionic strengths and media are reported in Table 1.

As can be seen in Table 1, the solubility of naringin in NaClO₄ is higher than those in NaCl. In particular, naringin exhibits a salting out effect in NaCl medium, being the solubility in water higher than those in sodium chloride. On the contrary, a salting in effect is observed when the inert salt is NaClO₄, the solubility increasing with the ionic strength. It was not possible to compare our results with literature data, whose are referred to measurements performed in non-aqueous solvent.^{21,22}

Potentiometric and mass spectrometric measurements

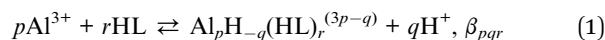
The metal (C_M) and ligand (C_L) concentrations were ranged from 0.5×10^{-3} to 1.5×10^{-3} mol L⁻¹. The upper limit was imposed by the low solubility of ligand under our experimental

Table 1 Solubility at 37.0 °C of naringin in water and in aqueous solutions of NaCl and NaClO₄ at different ionic strength. The uncertainties represent standard deviation

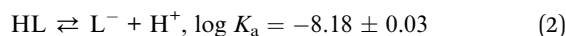
I , mol L ⁻¹	$S \times 10^3$, mol L ⁻¹
Pure water	1.015 \pm 0.002
0.16 NaCl	0.999 \pm 0.004
1.0 NaCl	0.932 \pm 0.004
3.0 NaCl	0.775 \pm 0.003
0.5 NaClO ₄	1.539 \pm 0.003
1.0 NaClO ₄	1.769 \pm 0.003
3.0 NaClO ₄	2.333 \pm 0.008



conditions. The ligand-to-metal ratio was varied between 1 and 3. The hydrogen ion concentration was ranged from $3.15 \times 10^{-3} \text{ mol L}^{-1}$ (pH 2.5) to incipient precipitation of basic salts which takes place in the range $[\text{H}^+] = 0.32\text{--}0.032 \times 10^{-3} \text{ mol L}^{-1}$ (pH 3.5–4.5) depending on the specific ligand-to-metal ratio. The general equilibrium can be written as follows:



which takes into account the possible formation of simple ($q = r$), mixed ($q \neq r$), mononuclear ($p = 1$) and polynuclear ($p > 1$) species. The most probable p , q and r values and the corresponding constants β_{pqr} were obtained by a least squares fitting of the potentiometric data.³³ In the numerical treatments, the acidic constant of naringin (equilibrium 2), determined by potentiometric measurements under the same experimental conditions (*i.e.*, 37.0 °C and in 0.16 mol L⁻¹ NaCl) in the absence of metal ion, was maintained invariant:



the uncertainty on this constant represents 3σ . The reproducibility and reversibility of the latter equilibrium were verified by performing titrations in acidic and in alkaline directions. No attempts were made to evaluate the second acidic constant due to the ligand oxidation reaction which occurs at a pH value greater than 8.5. Like many other cations, Al^{3+} can be hydrolysed to form solutions of mononuclear as well as polynuclear hydroxide complexes which can be stable indefinitely. The species $\text{Al}(\text{OH})_2^+$ and $\text{Al}(\text{OH})_2^+$ were considered the predominant hydrolysis products under our experimental conditions.³⁴ The relative equilibrium constants were taken from literature¹⁸ and were unchanged during the numerical evaluation, whose details are reported below (Table 2). Experimental data comprised 4 titrations with 78 data points.

The complexes of $\text{Al}(\text{III})$ with naringin were characterized by the (1,–1,1) and (1,–3,1) stoichiometries. No other species, introduced to improve the fit, was retained. In order to visualize our results, the refined equilibrium constants were used to represent the distribution of Al^{3+} in the different species (Fig. 1). All proposed species reached concentration levels no lower than 25% with respect to the total metal amounts. Consequently, meaningful concentrations were obtained for each species, allowing a correct definition of the respective equilibrium

Table 2 Survey of the $\log \beta_{pqr} \pm (3\sigma)$, according to the general equilibrium 1, for aluminium(III)–naringin complexes obtained by numerical procedure

(p,q,r)	$\log \beta_{pqr} \pm 3\sigma$
(1,–1,1)	1.01 ± 0.09
(1,–3,1)	-8.2 ± 0.2
σ	0.30
χ^2	4.28
U	3.14

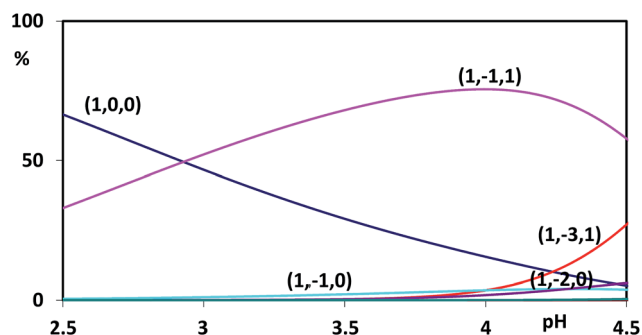


Fig. 1 Distribution diagram of aluminium cation in the presence of naringin ($C_M = 0.5 \times 10^{-3} \text{ mol L}^{-1}$ and $C_L = 1.5 \times 10^{-3} \text{ mol L}^{-1}$).

constants. In the whole pH range investigated the predominant species is the complex with stoichiometry (1,–1,1), while the species with (1,–3,1) stoichiometry reaches significant percentages at a less acidic pH range (from 4.0 to 4.5). As can be seen the species generated by the metal hydrolysis reach concentration levels no higher than 10% confirming that the sequestering ability of naringin towards $\text{Al}(\text{III})$ is competitive with water.

To gain additional insight on the complexes formation, we have compared the UV-vis spectra of the free and bound ligand (Fig. 2). The naringin absorption spectrum displayed three bands (*i.e.*, 330, 282 and 225 nm); with an increase on metal cation concentration the absorption maxima were red shifted (385 and 307 nm) indicating that the complexation occurs. The bathochromic shift in the absorption spectra confirms that deprotonation takes place at the hydroxyl group which gives red shifted absorption and maxima.

Mass spectrometric methodologies provide a rapid and sensitive tool for the identification and characterization of the species in terms of structure and stoichiometry.^{35,36} Therefore, the equilibrium behaviour and the speciation models were verified by analysing a naringin–aluminium solution, at pH 3.5 and in a stoichiometric ratio 1 : 1, with mass spectrometry in aqueous medium. The mass spectrum of the ions generated in source by ESI shows different species (Fig. 3). In particular, the molecular ions at m/z 1185 and m/z 623 correspond, respectively, to the aluminium complex bound to two and one molecules of deprotonated naringin. The further tandem mass spectrometry experiment performed on the isolated species at m/z 1185 shows a clear fragmentation pattern (Fig. S1†): the ion

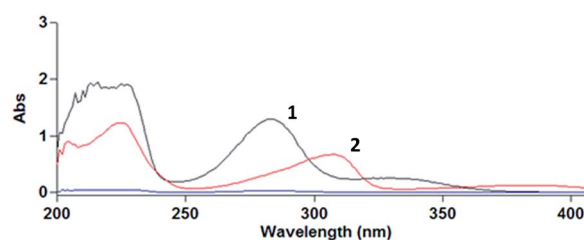


Fig. 2 UV-vis spectra of the free ligand $0.1 \times 10^{-3} \text{ mol L}^{-1}$ (line 1) and of the complexes formed between naringin and $\text{Al}(\text{III})$ $0.1 \times 10^{-3} \text{ mol L}^{-1}$ (line 2).



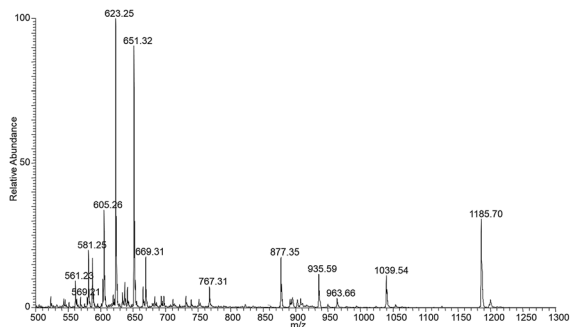


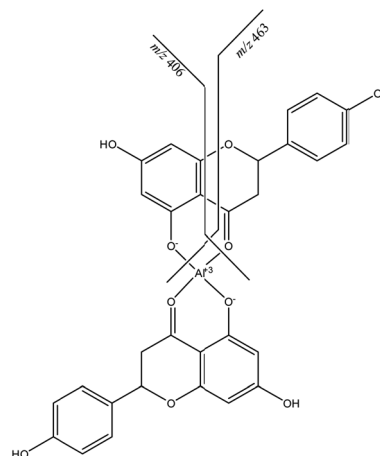
Fig. 3 ESI (+) MS spectrum of stable ion of the naringin–aluminium solution.

at m/z 1039 corresponds to the formal loss of one rhamnose unit from a naringin moiety, which subsequently fragment at the aglycon site generating the species at m/z 877 (loss of glucose unit).

Other diagnostic ions are those at m/z 731 and m/z 569, which are related to the loss of the rhamnose and glucose moieties from the second naringin molecule. The latter ion, present also as minor signal in the spectrum of stable ions (Fig. 3) and which contains two molecules of the aglycon naringenin linked to Al, indicates that the complexation site is on the aglycon moiety. By performing a MS/MS experiment on this ion (Fig. 4), it is possible to observe a particular fragmentation that leads to the formation of two complementary ions at m/z 463 and m/z 406 (Scheme 2), which suggests that the complexation site is located on the β -hydroxy ketone moiety. The MS/MS spectrum of the other stable species at m/z 621, which correspond to the complex (1,–1,1) shows significant fragment species at m/z 605 [$M - L$]⁺, due to the loss of a formal unit of water, and m/z 459, which is generated by the subsequent loss of the rhamnose unit (Fig. S2[†]).

By combining results from potentiometric and MS measurements we can assume that, according to the stoichiometric coefficients (1,–1,1) and (1,–3,1), the structure of these species is AlL^{2+} and $Al(OH)_2L$, respectively, the other coordination sites of aluminium being occupied by water molecules.

No comparison with the literature data was possible. The only evaluation concerns the interactions between naringin and



Scheme 2 Fragmentation of the ion at m/z 569.

other metal ions.^{37–39} In particular, as concern iron(III) ions, the formation of a single species of 1 : 1 stoichiometric ratio is studied from a kinetic point of view. Therefore, only a qualitative comparison between this data and our results is possible. The iron(III)–naringin complex contains a stable six-membered ring, according to the structure proposed for the aluminium–naringin complexes (Scheme 2).

Conclusions

In this study, the first under physiological conditions, the complexation of naringin with the Al(III) ion is reported. The speciation models and the formation constants proposed on the basis of potentiometric results were in agreement with Al(III)–naringin system MS data. The latter provided information regarding the structure of the complexes. From our results the following conclusions can be drawn:

- an accurate speciation study of this system by potentiometric measurements allowed us to clearly identify the stoichiometry of the complexes. This was the starting point necessary for understanding the relative structures;
- in the pH range investigated complexes with 1 : 1 stoichiometric ratio between aluminium and naringin, *i.e.*, AlL^{2+} and $Al(OH)_2L$, are possible;
- in agreement with previous data⁶ the complex formation induces a bathochromic shift of the UV-vis absorption bands;
- as confirmed by mass spectrometry results the complexation site is located on the β -hydroxy ketone moiety.

Conflicts of interest

There are no conflicts to declare.

Acknowledgements

This research was supported by University of Calabria.

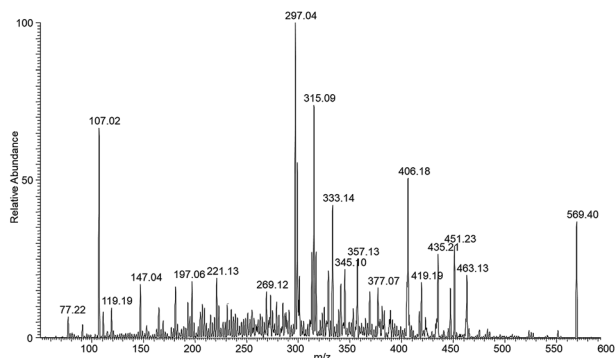


Fig. 4 ESI (+) Tandem mass spectrum on the isolated species at m/z 569.



Notes and references

- 1 M. G. L. Hertog, E. J. M. Feskens, P. C. H. Hollman, M. B. Katan and D. Kromhout, *Lancet*, 1993, **342**, 1007–1011.
- 2 C. S. Yang and Z.-Y. Wang, *J. Natl. Cancer Inst.*, 1993, **85**, 1038–1049.
- 3 M. R. Sowers, S. Crawford, D. S. McConnell, J. F. Randolph, E. B. Gold, M. K. Wilkin and B. Lasley, *J. Nutr.*, 2006, **136**, 1588–1595.
- 4 G. J. Soleas, L. Grass, P. D. Josephy, D. M. Goldberg and E. P. Diamandis, *Clin. Biochem.*, 2006, **39**, 492–497.
- 5 G. Mantovani, A. Maccio, C. Madeddu, G. Gramignano, M. R. Lusso, R. Serpe, E. Massa, G. Astara and L. Deiana, *Cancer Epidemiol., Biomarkers Prev.*, 2006, **15**, 1030–1034.
- 6 R. M. S. Pereira, N. E. D. Andrades, N. Paulino, A. C. H. F. Sawaya, M. N. Eberlin and M. C. Marcucci, *Molecules*, 2007, **12**, 1352–1366.
- 7 F. Billes, I. Mohammed-Ziegler, H. Mikosch and E. Tyihák, *Spectrochim. Acta, Part A*, 2007, **68**, 669–679.
- 8 M. M. Kasprzak, A. Erxleben and J. Ochocki, *RSC Adv.*, 2015, **5**, 45853–45877.
- 9 X. Deng, Z. Wang, J. Liu, S. Xiong, R. Xiong, X. Cao, Y. Chen, X. Zhenga and G. Tang, *RSC Adv.*, 2017, **7**, 38171–38178.
- 10 A. Garg, S. Garg, L. J. D. Zaneveld and A. K. Singla, *Phytother. Res.*, 2001, **15**, 655–669.
- 11 D. Susanti, H. M. Sirat, F. Ahmad, R. M. Ali, N. Aimi and M. Kitajima, *Food Chem.*, 2007, **103**, 710–716.
- 12 S. Kanno, A. Tomizawa, T. Ohtake, K. Koiwai, M. Ujibe and M. Ishikawa, *Toxicol. Lett.*, 2006, **166**, 131–139.
- 13 H. Ccedilelik, M. Kosar and E. Arinc, *Toxicology*, 2013, **308**, 34–40.
- 14 E. Furia and R. Porto, *J. Chem. Eng. Data*, 2008, **53**, 2739–2745.
- 15 E. Furia, A. Napoli, A. Tagarelli and G. Sindona, *J. Chem. Eng. Data*, 2013, **58**, 1349–1353.
- 16 E. Furia, D. Aiello, L. Di Donna, F. Mazzotti, A. Tagarelli, H. Thangavel, A. Napoli and G. Sindona, *Dalton Trans.*, 2014, **43**, 1055–1062.
- 17 E. Furia, T. Marino and N. Russo, *Dalton Trans.*, 2014, **43**, 7269–7274.
- 18 A. Beneduci, E. Furia, N. Russo and T. Marino, *New J. Chem.*, 2017, **41**, 5182–5190.
- 19 E. Furia, *J. Solution Chem.*, 2017, **46**, 1596–1604.
- 20 E. Finotti and D. Di Majo, *Nahrung*, 2003, **47**, 186–187.
- 21 L. Zhang, L. Song, P. Zhang, T. Liu, L. Zhou, G. Yang, R. Lin and J. Zhang, *J. Chem. Eng. Data*, 2015, **60**, 932–940.
- 22 J. Zhang, P. Zhang, T. Liu, L. Zhou, L. Zhang, R. Lin, G. Yang, W. Wang and Y. Li, *J. Mol. Liq.*, 2015, **203**, 98–103.
- 23 C. Exley, *Environ. Sci.: Processes Impacts*, 2013, **15**, 1807–1816.
- 24 F. Crea, P. Crea, C. De Stefano, O. Giuffrè, A. Pettignano and S. Sammartano, *J. Chem. Eng. Data*, 2004, **49**, 658–663.
- 25 L. Di Donna, H. Benabdelkamel, D. Taverna, S. Indelicato, D. Aiello, A. Napoli, G. Sindona and F. Mazzotti, *Anal. Bioanal. Chem.*, 2015, **407**, 5835–5842.
- 26 F. Mazzotti, L. Di Donna, A. Napoli, D. Aiello, C. Siciliano, C. M. Athanassopoulos and G. Sindona, *J. Mass Spectrom.*, 2014, **49**, 802–810.
- 27 S. K. Singh, A. Kundu and N. Kishore, *J. Chem. Thermodyn.*, 2004, **36**, 7–16.
- 28 A. Soto, A. Arce and M. K. Khoshkbarchi, *J. Solution Chem.*, 2004, **33**, 11–21.
- 29 S. R. Poulson, R. R. Harrington and J. I. Drever, *Talanta*, 1998, **48**, 633–641.
- 30 A. J. Queimada, F. L. Mota, S. P. Pinho and E. A. Macedo, *J. Phys. Chem. B*, 2009, **113**, 3469–3476.
- 31 A. Osol and M. Kilkpatrick, *J. Am. Chem. Soc.*, 1933, **55**, 4430–4440.
- 32 E. Furia, M. Falvo and R. Porto, *J. Chem. Eng. Data*, 2009, **54**, 3037–3042.
- 33 P. Gans, A. Sabatini and A. Vacca, *J. Chem. Soc., Dalton Trans.*, 1985, **6**, 1195–1200.
- 34 C. F. Baes and R. E. Mesmer, *The Hydrolysis of Cations*, Wiley Interscience, New York, 1976.
- 35 D. Aiello, S. Materazzi, R. Risoluti, H. Thangavel, L. Di Donna, F. Mazzotti, F. Casadonte, C. Siciliano, G. Sindona and A. Napoli, *Mol. Biosyst.*, 2015, **11**, 2373–2381.
- 36 A. Napoli, D. Aiello, G. Aiello, M. S. Cappello, L. Di Donna, F. Mazzotti, S. Materazzi, M. Fiorillo and G. Sindona, *J. Proteome Res.*, 2014, **13**, 2856–2866.
- 37 S. Nafisi, M. Hashemi, M. Rajabi and H. A. Tajmir-Riahi, *DNA Cell Biol.*, 2008, **27**(8), 433–442.
- 38 H. Rimac, Ž. Debeljak, D. Šakić, T. Weitner, M. Gabričević, V. Vrček, B. Zorc and M. Bojić, *RSC Adv.*, 2016, **6**, 75014–75022.
- 39 M. J. Hynes and M. O'Coinceanainn, *J. Inorg. Biochem.*, 2004, **98**, 1457–1464.

